ChemComm

COMMUNICATION

View Article Online
View Journal | View Issue

Spectroelectrochemistry of Fe^{III}- and Co^{III}-mimochrome VI artificial enzymes immobilized on mesoporous ITO electrodes†

Cite this: *Chem. Commun.*, 2014, **50**, 1894

Received 6th November 2013,
Accepted 3rd December 2013

DOI: 10.1039/c3cc48489k

www.rsc.org/chemcomm

R. Vitale,[a] L. Lista,[a] S. Lau-Truong,[b] R. T. Tucker,[c] M. J. Brett,[cd] B. Limoges,[e] V. Pavone,[a] A. Lombardi*[a] and V. Balland*[e]

UV-visible absorption spectroelectrochemistry elucidated the different redox behaviours of Fe^{III}- and Co^{III}-mimochrome VI artificial enzymes, adsorbed on mesoporous conductive films of ITO. The reduction of the ferric complex was rapid and reversible, while the cobaltic complex exhibited irreversible processes probably related to multiple coordination states.

The design of peptide-based synthetic metalloenzymes requires the adequate combination of both metal cofactors and protein chemistries, which can mutually modulate their functional properties.[1] This idea was the basis for the construction of the protein mimetic mimochrome VI (MC-6), a covalent deuteroporphyrin–peptide system, with two α-helical peptides embracing the porphyrin in a sandwiched structure (Fig. 1).[1–3]

MC-6 peptide chains were designed to (i) impart an asymmetry, in the first and second coordination shells, and (ii) stabilize the five-coordination. The spectroscopic and functional characterization of the Fe^{III}-MC-6 complex confirmed the correctness of the design. Fe^{III}-MC-6 exhibits a peroxidase-like catalytic activity with high stability under turnover conditions.[3]

More recently, we explored Co^{III}-MC-6 coordination by UV-visible (UV-vis) spectroscopy, highlighting similarities with coboglobins, cobalt reconstituted cytochrome *c*, and *N*-acetyl-Co^{III}-MP-8.[4–7] However, based on its absorption spectra, the Co^{III}-MC-6 coordination mode is not completely clear and further studies are needed.

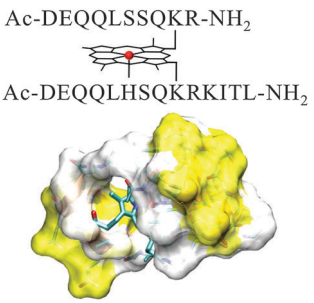

Fig. 1 Surface representation of the MC-6 model, with the amino acid sequence. The two main polar regions are shown in yellow.[3]

Due to their catalytic properties, Fe^{III}- and Co^{III}-MC-6 complexes offer the chance to construct new electrocatalytically active surfaces, with potential applications in the field of sensors or heterogeneous catalysis. Their development requires the (i) immobilization of MC-6 catalysts on conductive surfaces without significant structural perturbation, and (ii) the characterization of the resulting redox- and electrocatalytically-active surface by appropriate electroanalytical techniques. In this respect, the selection of advanced conductive matrices is crucial. Nanostructured films of tin-doped indium oxide (ITO) are very promising materials both for sensing and catalytic applications, thanks to their high surface area and excellent electrical and optical properties.[8] Their high transparency in the visible range allows characterization of immobilized redox biomolecules by various techniques (*i.e.* UV-vis or resonance Raman spectroscopies), deepening insight into the catalytic centre at the electrode surface. Furthermore, they can be exploited to develop innovative real-time spectroelectrochemical methods to study redox proteins or enzymes, and also biomimetic catalysts or artificial enzymes.[9–11]

Here, we report the immobilization of both Fe^{III}-MC-6 and Co^{III}-MC-6 on 1 μm-thick nanocrystalline mesoporous ITO films. These electrodes, prepared by GLAD (Glancing Angle Deposition), were recently successfully used for the immobilization and the spectroelectrochemical investigation of both heme-peptides and heme-proteins.[9–11] The modification of GLAD ITO electrodes was achieved by soaking them in 50 μM MC-6 (10 mM MES buffer, pH 6.5).

[a] *Department of Chemical Sciences, Complesso Universitario Monte S. Angelo, University of Naples "Federico II", Via Cintia, 80126 Naples, Italy. E-mail: alombard@unina.it*
[b] *ITODYS, UMR CNRS 7086, Université Paris Diderot, Sorbonne Paris Cité, 15, rue Jean-Antoine de Baïf, 75205 Paris Cedex 13, France*
[c] *Electrical and Computer Engineering, University of Alberta, Edmonton, Alberta, Canada T6G 2V4*
[d] *NRC National Institute for Nanotechnology, Edmonton, Alberta, Canada T6G 2M9*
[e] *Laboratoire d'Electrochimie Moléculaire, Université Paris Diderot, UMR CNRS 7591, 15, rue Jean-Antoine de Baïf, 75205 Paris Cedex 13, France. E-mail: veronique.balland@univ-paris-diderot.fr*

† Electronic supplementary information (ESI) available. See DOI: 10.1039/c3cc48489k

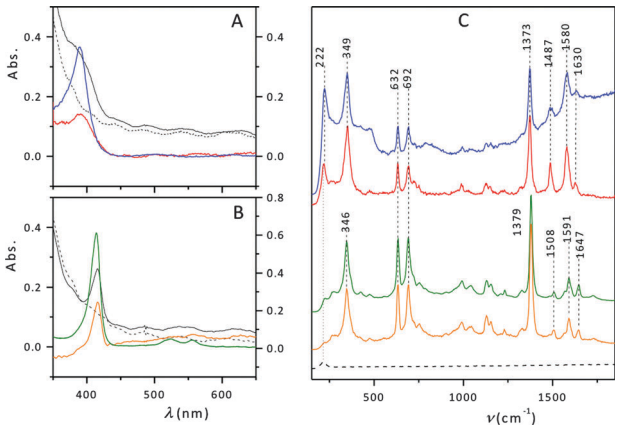

Fig. 2 UV-vis (A) and rR spectra (C) of Fe^{III}-MC-6 in solution (blue, C = 58 μM) and on ITO (red). The corresponding spectra for Co^{III}-MC-6 in solution (green, C = 54 μM) and on ITO (orange) are shown in (B) and (C). Raw and blank spectra are indicated in black, as full and dotted lines, respectively. All spectra were recorded in a 10 mM MES buffer at pH 6.5 (T = 20 °C). For solution spectra, 1 mm path length cells were used.

After equilibration (~14 hours), the electrodes were washed in a peptide-free MES buffer of high ionic strength (90 mM MES, 10 mM KPF_6, pH 6.5) to remove the fraction of poorly adsorbed molecules.

The resulting electrodes were first characterized by UV-vis spectroscopy. Once corrected from their blank ITO film absorption contribution, a clear and well-defined Soret band was detected at 390 nm and 418 nm for Fe^{III}-MC-6 and Co^{III}-MC-6, respectively (Fig. 2A and B). These wavelengths are similar to those obtained for the same complexes in solution, and indicate that the redox, spin and coordination sates of the metal ions are not strongly affected by their physical adsorption onto the metal oxide surface (Tables S1 and S3, ESI†).

In order to further study the coordination mode of the metal ions, the ferric and cobaltic complexes were investigated by resonance Raman, rR (Fig. 2C). The high quality rR spectra obtained over a large range of frequencies confirm the molecular and structural identity of the immobilized complexes with those in solution. Accordingly, the molar extinction coefficients of the immobilized MC-6 compounds were assumed to be equal to that determined in solution, *i.e.*, ε_{390} = 63 mM^{-1} cm^{-1} and ε_{416} = 113 mM^{-1} cm^{-1} for Fe^{III}-MC-6 and Co^{III}-MC-6, respectively. Using these values, the MC-6 surface concentration (Γ) was estimated 1–2 × 10^{-9} mol cm^{-2} was estimated. According to the ~66-fold surface enhancement, determined for a 1 μm-thick GLAD ITO electrode, the Γ value is close to that expected for a monolayer covering the overall specific surface area of the porous metal oxide. The Γ value is also in agreement with that previously obtained with a saturated monolayer of adsorbed Fe^{III}-MC-6 on decan-1-thiol-modified gold electrodes.[2]

The adsorption kinetics of Fe^{III}-MC-6 within the mesoporous ITO film was explored by plotting the Soret band absorbance as a function of soaking time (Fig. S1, ESI†). A first-order adsorption rate constant was determined (k_{ads} = 0.14 min^{-1}). An analogous value was reported for MP-11 adsorption on similar ITO electrodes.[11] It suggests a high affinity of Fe^{III}-MC-6 for the hydrophilic ITO film, thanks to the presence of several polar amino acid residues (Fig. 1), and a rapid saturation of the porous metal oxide surface after 30 min of immersion. Only ~10% desorption was observed at high ionic strength, while the remaining 90% remained stable over hours.

In the Fe^{III}-MC-6 rR spectra, the ν_4 and ν_3 oxidation marker bands are found at 1373 and 1487 cm^{-1}, respectively, as expected for 5-coordinated high spin (HS) ferric complexes.[12] In contrast, the ν_2 spin state marker band is observed at 1580 cm^{-1}, a frequency characteristic of 6-coordinated low-spin complexes (LS) (Table S2, ESI†).[13,14] This could be due to the structural differences between MC-6 deuteroporphyrin and natural heme-protein protoporphyrin, but it may also be indicative of a spin-state admixture (S = 3/2, 5/2 or QS state), in agreement with Maltempo's quantum mechanical theory.[15] Several class III peroxidases, cytochrome c', and heme-models were described using this model, on the basis of their rR, EPR, NMR, and UV-vis spectra.[12,16–19]

In the case of Co^{III}-MC-6, ν_4, ν_3 and ν_2 rR marker bands were found at 1379, 1508 and 1591 cm^{-1}, respectively. These wavenumbers are similar to those reported for 6-coordinated low spin bis-pyridine Co^{III}-porphyrins and for oxy-cobaltous-globins (Table S4, ESI†).[20,21] Accordingly, they may be indicative of a 6-coordinated low spin complex. However, it is difficult to definitely assign spin and coordination states to Co^{III}-MC-6, due to the lack of reference rR data on 5-coordinated cobaltic porphyrin complexes. Hence, the use of multiple and combined analytical techniques, *e.g.* spectroscopic and spectroelectrochemical, is desirable to gain deeper insight into Co^{III}-MC-6.

UV-vis spectroelectrochemistry allows for easy detection of the M^{III}/M^{II} interconversion during a potential-step redox titration or cyclic voltabsorptometric experiments (Fig. 3). When a constant cathodic potential was applied to the MC-6-modified ITO electrodes, the UV-vis spectra of the fully reduced species were obtained. The positions of Co^{II}- and Fe^{II}-MC-6 Soret bands were reasonably coincident with those

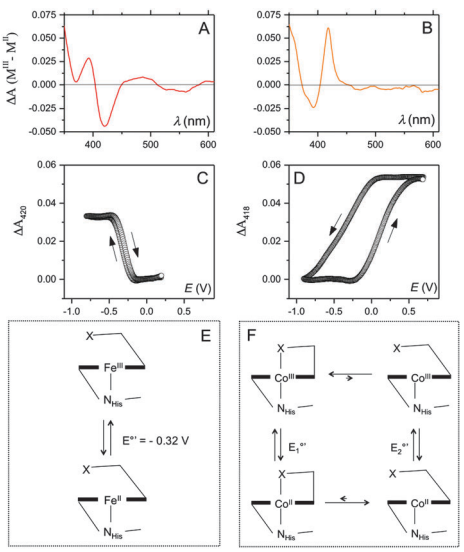

Fig. 3 UV-vis difference spectra obtained for (A) Fe^{III}-MC-6-ITO and (B) Co^{III}-MC-6-ITO, when the applied reducing potentials are −0.5 V, and −0.9 V, respectively. CVAs recorded at 0.01 V s^{-1} of (C) Fe^{III}-MC-6-ITO, and (D) Co^{III}-MC-6-ITO (λ = 420 nm and λ = 418 nm are indicative of Fe^{II}-MC-6 increase and Co^{III}-MC-6 decrease, respectively). Integration time: 10 ms; experimental conditions: 90 mM MES buffer, 10 mM KPF6 pH 6.5; T = 20 °C. Bottom schemes: (E) a simple E.T. mechanism observed for Fe^{III}-MC-6 and (F) a square-scheme mechanism suggested for Co^{III}-MC-6.

obtained in solution. In particular, the Fe^{II}-MC-6 spectra were fully consistent with a high-spin 5-coordinated Fe^{II} having an axial histidine at the fifth coordination site.[3] At the same time, spectra of Co^{II}-MC-6 revealed quite a good agreement with a planar low spin Co^{II}-complex having a single axially coordinated nitrogen base (Tables S1–S3, ESI†).[4,5] Difference absorption spectra of both MC-6-ITO show well resolved M^{III} (λ_{Fe} = 392 nm, λ_{Co} = 418 nm) and M^{II} (λ_{Fe} = 420 nm, λ_{Co} = 390 nm) contributions (Fig. 3).

The potential-step redox titration of Fe^{III}-MC-6-ITO was fully reversible, with two well-defined isosbestic points at 403 and 450 nm (Fig. S2, ESI†). The resulting titration curve was fitted to the Nernst equation from which an apparent standard potential of $E^{0\prime}$ = −0.32 V (*vs.* Ag/AgCl) and a value of n_{app} = 0.7 electron transferred were inferred. The $E^{0\prime}$ value is similar to the one determined for the molecule in solution or immobilized on a gold electrode, thus confirming that the redox properties of Fe^{III}-MC-6 remain unmodified upon adsorption.[2] The low n_{app} value, which should theoretically be equal to 1 for the one-electron Fe^{III}/Fe^{II} couple, may be due to the variable distribution of the artificial enzyme in (i) different orientations on the surface and/or (ii) diverse chemical microenvironments, as previously reported.[11]

Fe^{III}-MC-6-ITO cyclic voltabsorptometry evidences a typical thin-layer redox behaviour process since, at low scan rates (ν), (i) the sigmoidal plots of reduction and oxidation in the cyclic voltabsorptogram (CVA) are almost superimposed (Fig. 3), (ii) the anodic and cathodic waves in cyclic voltammetry (CV) are highly symmetric, showing a peak potential difference relatively close to 0 (Fig. S3, ESI†), and (iii) the cathodic and anodic peak intensities are a linear function of ν, up to 0.1 V s^{-1} (Fig. S4, ESI†). As the scan rate is further increased, the hysteresis between the reduction and oxidation curves is enlarged, indicating an increased kinetic control of the redox process by the heterogeneous electron transfer rate ($\sim$4 s^{-1}).

In contrast to the relatively well-defined reversible one-electron transfer process observed with Fe^{III}-MC-6, the CVA of Co^{III}-MC-6-ITO shows a large hysteresis between the reduction and oxidation processes (*e.g.* ΔE_p = 0.5 V at ν = 0.01 V s^{-1}) (Fig. 3).

In CV, such a sluggish redox process was very difficult to identify due to the large capacitive background current (Fig. S3, ESI†), thus explaining the pertinence and advantage of using a spectroelectrochemical method, which is totally free of these capacitive background current responses.

Attempts to diminish or suppress the oxidation–reduction hysteresis by decreasing the scan rate were proved to be unsuccessful. The large hysteresis reported here is thus indicative of a square scheme mechanism involving fast and irreversible chemical processes coupled to the preceding electron transfer (E.T.) reactions.

Similar phenomena were reported for the base-off–base-on equilibrium in vitamin B12, and the E.T. associated to a large conformational change found in cytochrome *cd*1.[22,23] In vitamin B12, breaking of intramolecular ligand coordination occurred upon Co^{II}/Co^{I} reduction, resulting in a large potential difference between the reduction and the oxidation waves in CV, at an appropriate scan rate.[22]

In analogy, binding–unbinding of an intramolecular sixth ligand could be associated with a large structural reorganization of the peptide conformation in the Co^{III}-MC-6 complex (Fig. 3). This hypothesis is supported by the spectroscopic data recorded for the oxidized and reduced species, which are consistent with a low spin 6-coordinated Co^{III} ion and a 5-coordinated Co^{II} ion. Difference in the coordination mode of the Co^{III}- and Co^{II}-MC-6 is further supported by the low reduction potential reported for the Co^{III}/Co^{II} redox transition.[24] Since no exogenous ligand is present in solution, we assume that the sixth ligand comes from the distal peptide chain (*e.g.* Asp^1 or Glu^2 of the decapeptide).

In conclusion, the comparative spectroelectrochemical study of Fe^{III}- and Co^{III}-MC-6 adsorbed on mesoporous ITO electrodes reveals contrasting redox behaviours that seem to be related to different coordination modes in their oxidized states.

MC-6 was conceived to stabilize 5-coordinated complexes, since no ligand is supplied by the peptide on the deuteroporphyrin distal side. The present results indicate that conformational preferences of the peptide chains in Co^{III}- and Fe^{III}-MC-6 complexes might be different. This information could be exploited for the redesigning of MC-6 aimed at stabilizing a 5-coordinated Co^{III}.

The Italian Ministry of University and Scientific Research (PRIN 2007 KAWXCL) and the French Ministry of Foreign Affairs (fellowship to RV) supported this work. RTT and MJB acknowledge NSERC, AITF, Micralyne, Inc., and Killam Trust for support. Cost action CM1003 is also kindly acknowledged.

Notes and references

1 A. Lombardi, F. Nastri and V. Pavone, *Chem. Rev.*, 2001, **101**, 3165–3189.
2 A. Ranieri, S. Monari, M. Sola, M. Borsari, G. Battistuzzi, P. Ringhieri, F. Nastri, V. Pavone and A. Lombardi, *Langmuir*, 2010, **26**, 17831–17835.
3 F. Nastri, L. Lista, P. Ringhieri, R. Vitale, M. Faiella, C. Andreozzi, P. Travascio, O. Maglio, A. Lombardi and V. Pavone, *Chem.–Eur. J.*, 2011, **17**, 4444–4453.
4 L. C. Dickinson and C. W. Chien, *J. Biol. Chem.*, 1973, **248**, 5005–5011.
5 T. Yonetani, H. Yamamoto and G. V. Woodrow, *J. Biol. Chem.*, 1974, **10**, 682–690.
6 L. C. Dickinson and J. C. Chien, *Biochemistry*, 1975, **14**, 3526–3534.
7 H. M. Marques, *Dalton Trans.*, 2007, 4371–4385.
8 K. M. Krause, M. T. Taschuk, K. D. Harris, D. A. Rider, N. G. Wakefield, J. C. Sit, J. M. Buriak, M. Thommes and M. J. Brett, *Langmuir*, 2010, **26**, 4368–4376.
9 C. Renault, K. D. Harris, M. J. Brett, V. Balland and B. Limoges, *Chem. Commun.*, 2011, **47**, 1863.
10 D. Schaming, C. Renault, R. T. Tucker, S. Lau-Truong, J. Aubard, M. J. Brett, V. Balland and B. Limoges, *Langmuir*, 2012, **28**, 14065–14072.
11 C. Renault, C. P. Andrieux, R. T. Tucker, M. J. Brett, V. Balland and B. Limoges, *J. Am. Chem. Soc.*, 2012, **134**, 6834–6845.
12 R. Weiss, A. Gold and J. Terner, *Chem. Rev.*, 2006, **106**, 2550–2579.
13 T. G. Spiro and T. C. Strekas, *J. Am. Chem. Soc.*, 1974, **96**, 338–345.
14 F. Nastri, A. Lombardi, G. Morelli, C. Pedone, V. Pavone, G. Chottard, P. Battioni and D. Mansuy, *JBIC, J. Biol. Inorg. Chem.*, 1998, **3**, 671–681.
15 M. M. Maltempo, *Q. Rev. Biophys.*, 1976, **9**, 181–215.
16 A. Feis, B. D. Howes, C. Indiani and G. Smulevich, *J. Raman Spectrosc.*, 1998, **29**, 933–938.
17 B. D. Howes, C. B. Schiodt, K. G. Welinder, M. P. Marzocchi, J. G. Ma, J. Zhang, J. A. Shelnutt and G. Smulevich, *Biophys. J.*, 1999, **77**, 478–492.
18 B. D. Howes, N. C. Veitch, A. T. Smith, C. G. White and G. Smulevich, *Biochem. J.*, 2001, **353**, 181–191.
19 K. M. Kadish, K. M. Smith and R. Guillard, *The porphyrin handbook*, Academic Press, San Diego, 2000, vol. 6.
20 W. H. Woodruff, T. G. Spiro and T. Yonetani, *Proc. Natl. Acad. Sci. U. S. A.*, 1974, **71**, 1065–1069.
21 W. H. Woodruff, D. H. Adams, T. G. Spiro and T. Yonetani, *J. Am. Chem. Soc.*, 1975, **97**, 1695–1698.
22 D. Lexa and J. M. Saveant, *Acc. Chem. Res.*, 1983, **16**, 235–243.
23 A. Koppenhöfer, K. L. Turner, J. W. A. Allen, S. K. Chapman and S. J. Ferguson, *Biochemistry*, 2000, **39**, 4243–4249.
24 M. T. de Groot and M. T. M. Koper, *Phys. Chem. Chem. Phys.*, 2008, **10**, 1023.